Solid-State Modification of Isotactic Polypropylene (iPP) via Grafting of Styrene. I. Polymerization Experiments

F. Picchioni,[1] J. G. P. Goossens,[1] M. van Duin,[2] P. Magusin[3]

[1]*Department of Polymer Technology (SKT), Dutch Polymer Institute, Eindhoven University of Technology, P.O. Box 513, 5600 MB Eindhoven, The Netherlands*
[2]*DSM Research, P.O. Box 18, 6160 MD Geleen, The Netherlands*
[3]*Schuit Institute of Catalysis (SKA), Eindhoven University of Technology, P.O. Box 513, 5600 MB Eindhoven, The Netherlands*

Received 19 October 2002; accepted 4 December 2002

ABSTRACT: Grafting of vinyl monomers onto isotactic polypropylene (iPP) in the solid state, that is, below the melting point, displays several advantages over melt or solution grafting processes, such as negligible degradation of the iPP and absence of any solvent. The final properties of such iPP modifications or actually compatibilized PP blends are dependent on the dispersion of the new polymer into the iPP matrix, which is controlled to a large extent by the degree of grafting versus the amount of free homopolymer formed. In the present work, the solid-state modification of iPP by styrene has been investigated from the point of view of the monomer polymerization behavior. In order to determine the styrene conversion and the distribution of the newly formed PS phase along the radius of the iPP powder particles, the reaction products were characterized by infrared (FTIR) and Raman spectroscopy. Fractionation of the reaction products via selective solvent extraction allowed the determination of the grafting efficiency (Φ). It was shown that besides the grafted PS two additional types of PS are formed, that is, free PS homopolymer in the pores of the PP powder and free PS in the amorphous PP phase. Phi shows an optimum as a function of the feed peroxide composition and the feeding rate. © 2003 Wiley Periodicals, Inc. J Appl Polym Sci 89: 3279–3291, 2003

Key words: polyolefins; graft copolymers; solid-state polymerization; radical polymerization

INTRODUCTION

Grafting reactions carried out onto a solid polymer substrate have been widely studied because of the inherent simplicity of the process itself as well as the quite obvious technical and economic advantages in carrying out the process at low temperatures without using solvents.

One of the first studies[1–3] on solid-state grafting of styrene (St) onto PP involved the selective oxidation of PP films by ozone in order to insert peroxide groups along the backbone. The peroxidized PP was then simply immersed in a water solution of the monomer in the presence of a Fe^{2+}-triethylenetetramine chelate and an emulsifier. The presence of the Fe^{2+}-chelate was necessary to start the polymerization via a redox reaction (decomposition of peroxide groups). The PP must preventively be treated with iodine to remove hydroperoxide groups formed during the oxidation stage and not active in the graft polymerization of St. It was found that the production of PS homopolymer strongly depends on the amount of hydroperoxide groups on the PP backbone probably because of the initiation of St polymerization by hydroxyl radicals.

Although one of the main advantages of the solid-state grafting is the absence of solvents, small quantities may be used as interfacial agents in order to improve the grafting efficiency. For example, toluene was used[4–7] as interfacial agent in the solid-state graft polymerization of maleic anhydride (MA) onto iPP. For the first time, the polymer was used in the form of reactor powder instead of film or fiber, which results in an increase of the surface area accessible for grafting. From the analysis of the reaction products by means of wet chemical methods, ^{13}C-NMR and FTIR, it was possible to conclude that the grafting mechanism in the solid state is essentially the same as in the melt except for the β-elimination pathway, which is strongly suppressed in the solid-state process because of the lower temperature. In this way, degradation of the polymer is prevented and deterioration of the mechanical properties is avoided.

A detailed study on the solid-state radical grafting of MA onto iPP was carried out by Borsig et al.,[8,9] who impregnated iPP powder with a solution of the radical initiator in the monomer and then raised the temperature to start the reaction. Such a procedure allowed monomer conversions similar to those obtained in the melt. In addition, from a study on the dependence of the degree of grafting on the monomer (MA) concen-

Correspondence to: F. P. Picchioni (F.P.Picchioni@tue.nl).

Journal of Applied Polymer Science, Vol. 89, 3279–3291 (2003)
© 2003 Wiley Periodicals, Inc.

tration in a wide range of compositions, the authors concluded that the grafting yield can be controlled by the monomer amount in the feed.

Modification of iPP in the solid state is the basis of an industrial process developed by Montell in the early 1990s resulting in the commercialization of the so-called Hivalloy products.[10–19] The process[17] consists of contacting porous PP polymer particles with a free-radical initiator and a vinyl monomer at temperatures in the range of 60–125°C, while controlling the monomer addition rate in the range of 0.1–4.5 pph/min. The reaction is carried out in a batchlike reactor and in a nonoxidizing environment in order to avoid polymer degradation. The process is carried out with vinyl monomers, which are able to give homopolymerization, leading to the formation of both free and grafted polymer chains. As a result, a new polymeric phase is formed upon polymerization: the final properties of the obtained product are dependent on the chemical nature of this new phase and on its dispersion into the PP matrix. The modified iPP powder is subsequently melt processed (with addition of stabilizers, rubber, and/or inorganic fillers) to yield the final product.

The fundamental concepts of the solid-state grafting onto PP have been studied by Rätzsch et al.[20,21] Under the conditions of solid-state processing ($T \approx 100$°C), the β-scission reaction of iPP can be neglected, which is not the case for the melt processes usually carried out at approximately 200°C. In addition, the use of porous iPP allows transport of the monomer and initiator directly to the reaction site. This condition can be fulfilled as a result of the particular polymerization technology of propylene, which leads to the formation of multigrain structures with the diffusion of the monomer/initiator mixture being limited to the amorphous phase of iPP. In terms of the multigrain model, the authors were able to distinguish the transport process of the components in the following steps: diffusion in the pores of the PP grain, mass transfer from the gas phase to the surface of the microparticle, adsorption in the amorphous phase, and diffusion in the amorphous phase of the microparticle. By assuming that the PP grain is homogeneous, it is possible to study the diffusion of several components into the PP grain and to determine the value of effective diffusion constants.

These concepts have been used to develop an industrial process for the production of grafted iPP materials,[22–26] containing approximately 20 wt % of PS with an average grafting efficiency of 50%, that is, half of the PS chains are grafted onto PP. The process can simply be carried out in a batch mixer as well as in a fluidized bed reactor. The working temperature can be selected on the basis of diffusion studies of the components into the PP grains. Recently,[27] the possibility of a chemical control of the grafting efficiency, that is, the ratio between grafted and homopolymerized chains, at least in the case of the St grafting onto iPP, was reported. With the aim of reducing the overall amount of free-polystyrene, complexes of metals of the V–VIII groups with acetylacetonate (acac) were successfully added to the reaction mixture (monomer/radical initiator). Although the mechanism by which these compounds act has not been fully elucidated, it is possible to mention that in particular Mn(acac)$_3$, Cr(acac)$_3$, and Fe(acac)$_3$ were highly effective in suppressing the formation of PS homopolymer.

In this work the modification of iPP by St has been studied, aiming at the determination of the grafting efficiency as a function of the feed composition and the feeding rate, that is, the rate at which the monomer/initiator mixture is added to the solid iPP. In addition, a detailed spectroscopic characterization has been performed on the modified iPP powder particles in order to determine the distribution of the PS phase along the radius of the iPP particle.

EXPERIMENTAL

Materials

iPP was supplied by DSM Research (Yeleen, The Netherlands) in the form of a white powder (particle diameter of approximately 0.3 mm). It displayed a crystallinity of about 51 wt % at 90°C (reaction temperature), as determined by DSC.

St (Aldrich) containing 10–15 ppm of a radical inhibitor (4-*tert*-butylcatechol) was used without further purification. Chlorobenzene (Merck), *n*-octane (Aldrich), and dichloromethane (CH_2Cl_2; Merck) were used without further purification. The free radical initiator, 2,2′-azobis(2-methylpropionitrile) (AIBN) (Merck), was used as received.

Grafting reactions

The grafting reactions were carried out in a typical solid-state,[17,28] double-skinned reactor preheated to 90°C, equipped with a condenser and a mechanical stirrer. The stirrer consists of a steel rod having at one edge a Teflon anchor perfectly fitting into the cylindrical shape of the reactor and, consequently, being able to remove scraps, whenever formed, from the reactor wall. The reactor was also connected to a nitrogen inlet and a peristaltic pump by which the reactive mixture (St/AIBN) was pumped into the reactor at the desired rate. The feeding rate was calculated from the density of the reactive mixture, assumed to be approximately equal to the density of pure St, and the addition time. The flow rate is expressed, following the convention in the literature,[17] as pph/min: part per hundred of reactive mixture, with respect to the amount of iPP, per minute. In a graft polymerization experiment, the solid powder was introduced into the reactor and then stirred under a dry nitrogen flow (approximately 1 bar pressure) for 10 min in order to

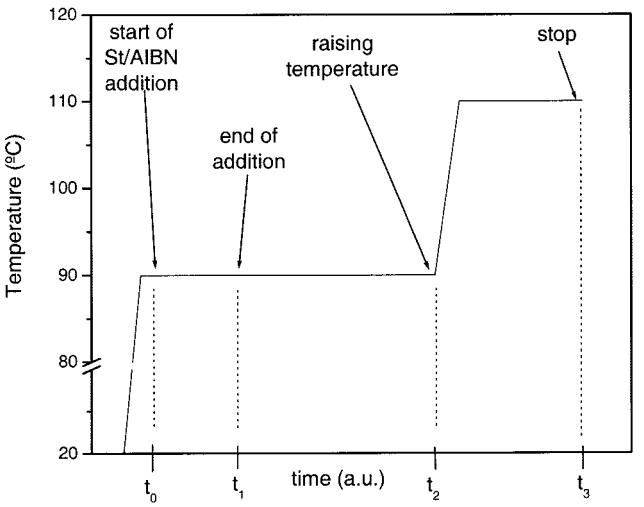

Scheme 1 Experimental temperature/time profile for a typical solid-state grafting experiment. $t_0 \rightarrow t_1$: addition step (dependent on addition rate). $t_1 \rightarrow t_2$: reaction step (40 min, i.e., four times the half-life time of AIBN at 90°C). $t_2 \rightarrow t_3$: annealing step (15 min).

remove any trace of oxygen. The temperature/time profile for a typical experiment is shown in Scheme 1. The addition of the St/AIBN mixture was started at the desired rate at 90°C for a total time (t_1) dependent on the final feed composition, that is, on the total volume of reactive mixture. The reaction was then continued for a fixed time of 40 min, corresponding to four times the half-life time of AIBN at 90°C. At this point (t_2) the temperature was raised to 110°C in approximately 5 min and maintained at this level for a total time of 10 min in order to decompose unreacted initiator molecules and to terminate the polymerization. The reaction was then stopped, and the product was immediately recovered from the reactor and stored at −4°C before further analysis.

Kinetic experiments

Kinetic experiments, aimed at the determination of the St conversion as a function of the reaction time, were performed according to the above-mentioned scheme except for the fact that samples of approximately 100 mg were taken from the reactor every 5 min and immediately quenched in liquid nitrogen.

Characterization techniques

Infrared spectroscopy

Samples for FTIR analysis were prepared by dissolving a small amount of the material in chlorobenzene followed by casting on dry KBr pellets. After fast evaporation of the solvent, the spectra were recorded on a Mattson FTIR instrument. The calibration curve for quantitative analysis, as depicted in Figure 1, was determined by recording spectra of iPP/PS blends prepared by simple dissolution of iPP and PS pellets in prefixed amounts in toluene. The experimental points were then fitted by a nonlinear method with an allometric-type function:

$$y = a \cdot x^b \tag{1}$$

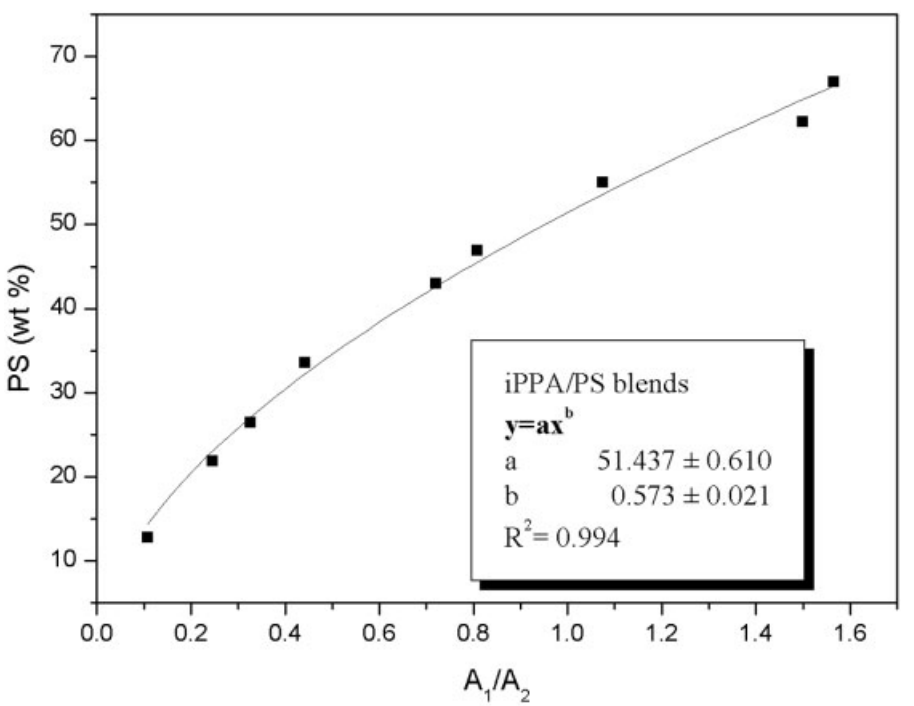

Figure 1 FTIR calibration curve for iPP/PS mixtures (fit results are given in the figure insert). A_1 = area of the peak at 700 cm^{-1}; A_2 = area of the peak at 1370 cm^{-1}.

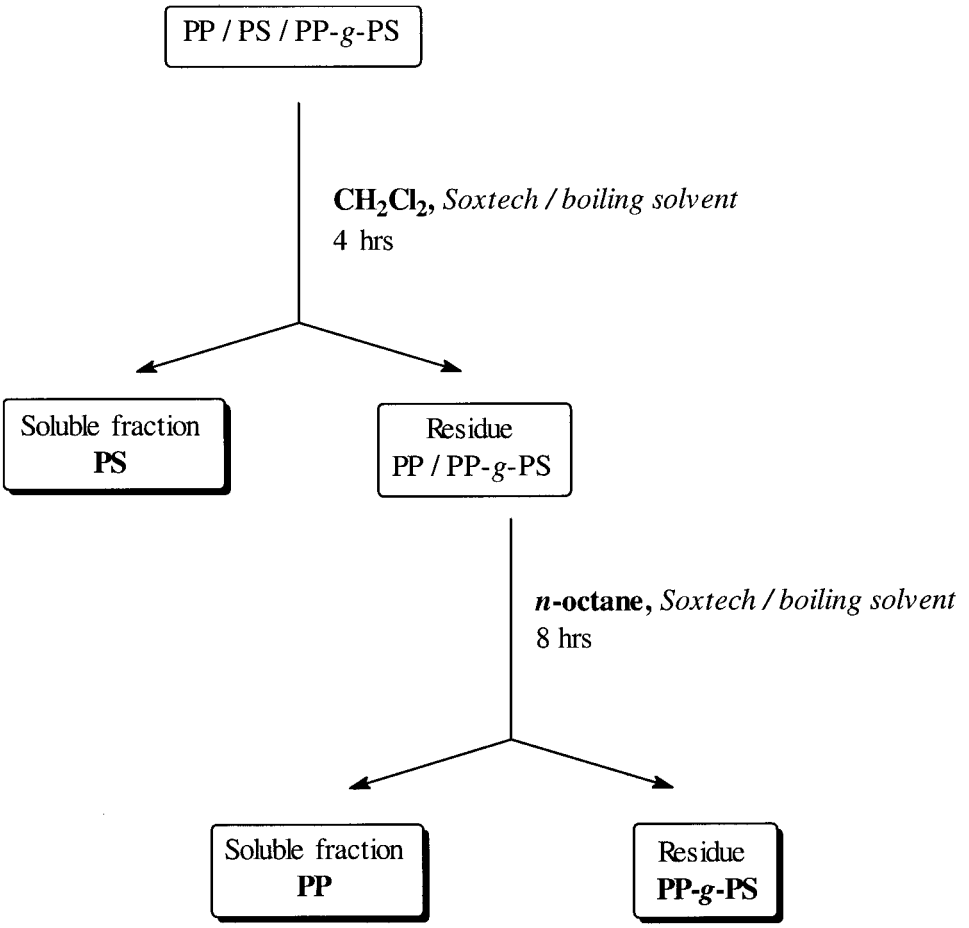

Scheme 2 Fractionation procedure: expected results.

where a and b are parameters to be determined by the fitting procedure, y is the weight percentage of PS in the sample, and x is the ratio between the peak area of the absorptions at 700 cm^{-1} (out-of-plane bending mode of the aromatic C—H) and 1370 cm^{-1} (bending mode aliphatic C—H). The fitting procedure was performed using the Origin 6.0 software of Microcal Origin ®.

The total PS content in the final product, as determined by FTIR, allows the calculation of the St conversion according to

$$\text{St conversion (\%)} = \frac{\text{amount of PS in the reaction product}(g)}{\text{amount of St in the starting mixture}(g)} \times 100 \quad (2)$$

Raman spectroscopy

Samples for Raman spectroscopy were prepared by embedding PP-modified powder particles in a commercial epoxy formulation, which was subsequently cured at room temperature. Cross-sections of single particles were obtained by cutting the embedded particles using a microtome and were analyzed by Raman spectroscopy using a Dilor Labram dispersive Raman spectrometer. The incident laser excitation line was 532 nm from a Nd:YAG laser source. A 10X magnification objective was combined with a confocal hole diameter of 1000 μm. This corresponds to a sample area close to 20 μm in diameter within a penetration depth of approximately 20 μm. The slit entrance of the detector was set to 300 cm^{-1}, which resulted in a spectral resolution of approximately 3 cm^{-1} using a grating with 1800 lines/mm. The spectra were obtained at two grating positions, one centered around 1200 cm^{-1} and one centered around 3000 cm^{-1} and were collected with accumulation times of 30 s.

Selective solvent extractions

The separation procedure consisted of two steps (Scheme 2):

1. Extraction with CH_2Cl_2: approximately 0.8 g of the reaction product, still in a powder form, was extracted in a Soxtech apparatus for 4 h at the solvent boiling temperature (40°C). Both the residue and the extracted fraction were then dried in a vacuum oven at 40°C to constant weight.

TABLE I
Graft Polymerization of Styrene onto iPP

Run	Experimental[a] iPP wt %	Sty wt %	AIBN wt % St	r_{add} pph/min	PS (wt %) ± error[b]
iPP13[c]	80	20	1.0	1.0	0.0
iPP16	70	30	0.0	1.0	0.0
iPP7	80	20	1.0	0.5	3.4 ± 2.7
iPP21	80	20	1.0	0.8	7.7 ± 2.5
iPP1, iPP14, iPP20	80	20	1.0	1.0	18.3 ± 1.2
iPP8	80	20	1.0	1.5	18.4 ± 1.5
iPP22	80	20	1.0	1.7	19.3 ± 2.1
iPP4, iPP15	80	20	1.0	2.0	14.6 ± 1.4
iPP24	80	20	1.0	2.5	14.2 ± 1.9
iPP9	70	30	0.5	1.0	15.7 ± 2.2
iPP12	70	30	0.8	1.0	13.6 ± 1.7
iPP2, iPP17, iPP23	70	30	1.0	1.0	28.4 ± 0.6
iPP11	70	30	1.2	1.0	28.9 ± 2.4
iPP18	70	30	1.3	1.0	23.0 ± 1.5
iPP10	70	30	1.5	1.0	23.8 ± 2.4
iPP19	70	30	2.0	1.0	25.7 ± 2.1
iPP27	70	30	3.0	1.0	23.1 ± 2.3

[a] The feed composition is expressed in wt % for iPP and styrene; the percentage of AIBN (wt %) is expressed relative to the styrene amount.
[b] 95% confidence limit.
[c] Carried out in air.

2. Extraction in *n*-octane: the dried residues from the CH_2Cl_2 extractions were directly extracted by *n*-octane vapors (boiling temperature of approximately 127°C) for 10 h using a Soxtech apparatus. Both the residue and extracted fraction were dried in a vacuum oven at 40°C to constant weight.

The selectivity of the separation procedure was checked both quantitatively (mass balance) and qualitatively (FTIR) on solution-cast and melt-processed (miniextruder; 200°C) iPP/PS blends. The mass balance is used to evaluate the grafting efficiency (Φ), which is defined as follows:

$$\Phi = \frac{\text{amount of grafted PS}(g)}{\text{amount of total formed PS}(g)} \times 100 \qquad (3)$$

In order to get an estimate of the efficiency of the separation procedure, a mass balance is used to calculate the extraction efficiency (Γ), defined as

$$\Gamma = \Gamma_{CH_2Cl_2} \times \Gamma_{n-oct} \qquad (4)$$

where Γ_x, that is, the extraction efficiency for solvent x, is defined as

$$\Gamma_x = \frac{\text{amount of extracted fraction}(g) + \text{amount of residue}(g)}{\text{total amount of material before extraction in x}(g)} \qquad (5)$$

Solid-state NMR

Proton-decoupled ^{13}C-NMR spectra were recorded on a Bruker DMX500 spectrometer operating at ^{1}H- and ^{13}C-NMR frequencies of 500 and 125 MHz, respectively. A 4 mm magic-angle-spinning (MAS) probehead was used with typical sample-rotation rates of 8 kHz. The radio-frequency power was adjusted to obtain 5 μs 90° pulses both for ^{1}H and ^{13}C nuclei. Adamantane was used for external calibration of the ^{13}C chemical shift. Proton spin-lattice relaxation in the laboratory and in the rotating frame, $T_1\{H\}$ and $T_{1\rho}\{H\}$, were measured for each of the polymer components separately via cross-polarization to the ^{13}C nuclei. The typical number of scans (NS) was 256, relaxation delays (D1) 5 s, and the number of experiments per relaxation data set (NE) 12.

Surface area measurements

Surface area measurements were performed by using an "indirect" BET method[29] consisting of the adsorption of krypton at 77 K. The apparatus used was an ASAP2000 from the Micromeritics Company (USA).

RESULTS AND DISCUSSION

To study the graft polymerization of St onto iPP, first a series of experiments was carried out by changing the feed composition, that is, by changing the ratio of the three starting components: iPP, St, and AIBN. In Table I all the experimental recipes are reported, to-

TABLE II
Reproducibility of the Polymerization Experiments

Couple of repeated experiments	Experimental t values	Theoretical t value
iPP20/iPP14	0.72	2.31
iPP4/iPP15	0.78	2.31

[a] Values were determined using t test.

gether with the employed rate of addition and the total PS content as determined by FTIR and calculated by using the calibration curve in Figure 1.

In order to study the homogeneity of the prepared samples at a microscopic level, the error of the determination of the PS content by FTIR was determined by recording several spectra of the same sample (iPP12). The recorded spectra allowed the calculation of the A_1/A_2 ratio and, consequently, the total PS content for every single FTIR spectrum. The average PS content for iPP12 was 13.6 ± 0.4 wt %, where the standard deviation (SD) from the mean value was assumed to be the absolute error. Assuming a confidence limit of 5%, it is possible to estimate[30,31] the error of the FTIR measurements (e_{FTIR}) according to

$$e_{FTIR} = SD \cdot f_{5\%} = 0.4 \cdot 2.1 \approx 0.9 \quad (6)$$

where $f_{5\%}$ is the theoretical coefficient for 95% confidence limit with 17 degrees of freedom (18 spectra recorded for iPP12).[30,31] The error of the average PS content (last column of Table I), determined according to the 95% confidence limit, is in any case significantly higher than the errors of the FTIR measurements, with the exception of the repeated runs iPP2, iPP17, and iPP23. This indicates that the samples are microscopically heterogeneous.

The reproducibility of the experiments was studied according to the theory of the t test.[30,31] Two couples of repeated experiments, iPP20/iPP14 and iPP4/iPP15, were carried out and the average PS content for each one of them was determined by recording several FTIR spectra. For each couple, the experimental variance (s^2) and the t value were then determined (Table II). For both couples, the experimental t values are lower than the theoretical t values for a confidence limit of 95% with eight degrees of freedom (which corresponds, in our case, to the determination of the PS content on nine different FTIR determinations). As a consequence, upon carrying out two equivalent experiments, the same results, in terms of total PS content, will be obtained (within the specified error limit) in 95% of all cases.

The first two reference experiments, iPP13 and iPP16, did not display the presence of any PS, clearly indicating that no polymerization took place in air (iPP13) or in the absence of the radical initiator (iPP16). The last result is particularly interesting when compared to some data in the literature,[32,33] which show the possibility of thermal St polymerization, in the absence of radical initiators at 90°C, both in bulk and in the presence of atactic polypropylene (aPP) under quiescent conditions. The opposite behavior observed when St is slowly added to iPP clearly shows the importance of diffusion in this kind of process. The thermal polymerization of St is initiated by a bimolecular reaction,[33] which represents the limiting step of the polymerization kinetics. It is reasonable to assume that in our case the fast diffusion of St during the addition step results in a low local monomer concentration, which prohibits the bimolecular initiation step.

On the other hand, the polymerization reaction may be influenced not only by the change in the feed composition, but also by the rate of addition of the St/AIBN mixture to iPP. In fact, the total PS content as a function of the addition rate (r_{add}) at a fixed feed composition (Fig. 2) shows a steep increase at $r_{add} = 1$ pph iPP/min. This increase may be explained by taking into consideration that at low r_{add} values the relative fast diffusion of the St/AIBN mixture is not balanced by the feeding rate (as suggested by the blank experiment iPP16), so that the local monomer concentration, and thus the polymerization rate, is very low. It was not possible to determine whether the observed curve really displays a broad maximum or generally tends to an asymptotic value very close to 100% conversion at high values of r_{add}. This difficulty is not only connected to the experimental error in the PS determination, but also to nonhomogeneous conditions at high r_{add} values. Formation of PP powder lumps and scraps on the reactor wall was observed for high r_{add} values and even complete reactor fouling was noticed for very high values.

The plot of the total PS content as a function of the AIBN concentration (Fig. 3) at a fixed iPP/St ratio 70/30 wt/wt displays some important features: a maximum in conversion is observed at around 1 wt %

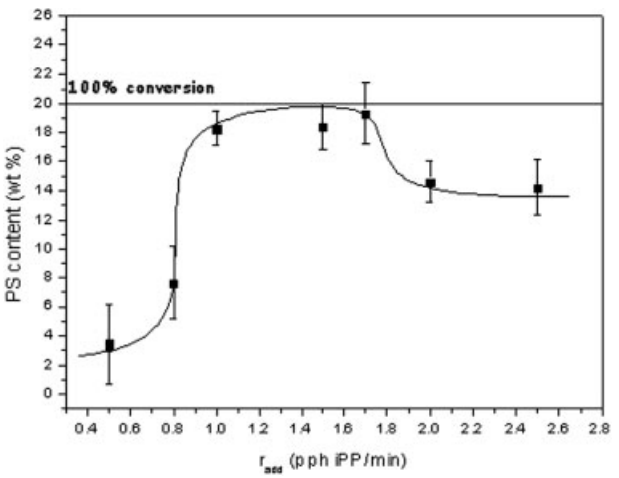

Figure 2 Total PS content as a function of addition rate (r_{add}). iPP/St (80/20 wt/wt), AIBN 1 wt % St.

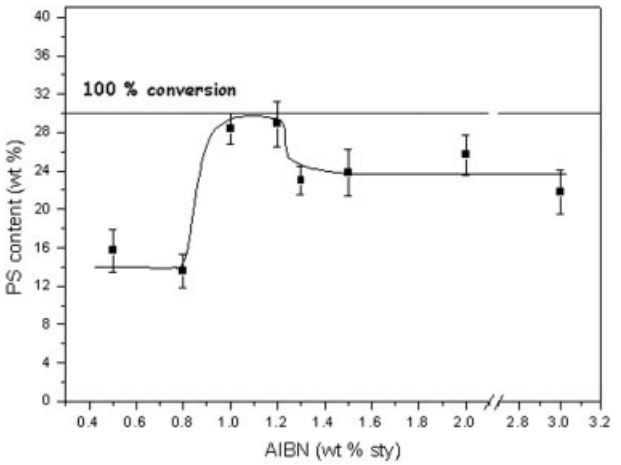

Figure 3 Total PS content as function of AIBN concentration in feed. iPP/St 70/30 wt/wt, r_{add} = 1 pph/min iPP.

of AIBN with respect to the St content, after which the conversion slowly decreases; 100% conversion is not reached, in contrast to some model systems,[32] for which, under quiescent conditions, a nearly quantitative formation of PS was observed.

The different behavior of the St polymerization under quiescent and stirred conditions, especially for low AIBN contents, may be related, once more, to the peculiar characteristics of the slow addition rate of the monomer/AIBN mixture to the iPP. This seems, like in the case of the blank run iPP16, to limit the polymerization itself. On the other hand, the small decrease of the PS content at high AIBN values represents a marked difference with the bulk polymerization of St initiated by AIBN, for which this decrease takes place at a much higher rate.[34] One possible explanation for this difference may be the presence of

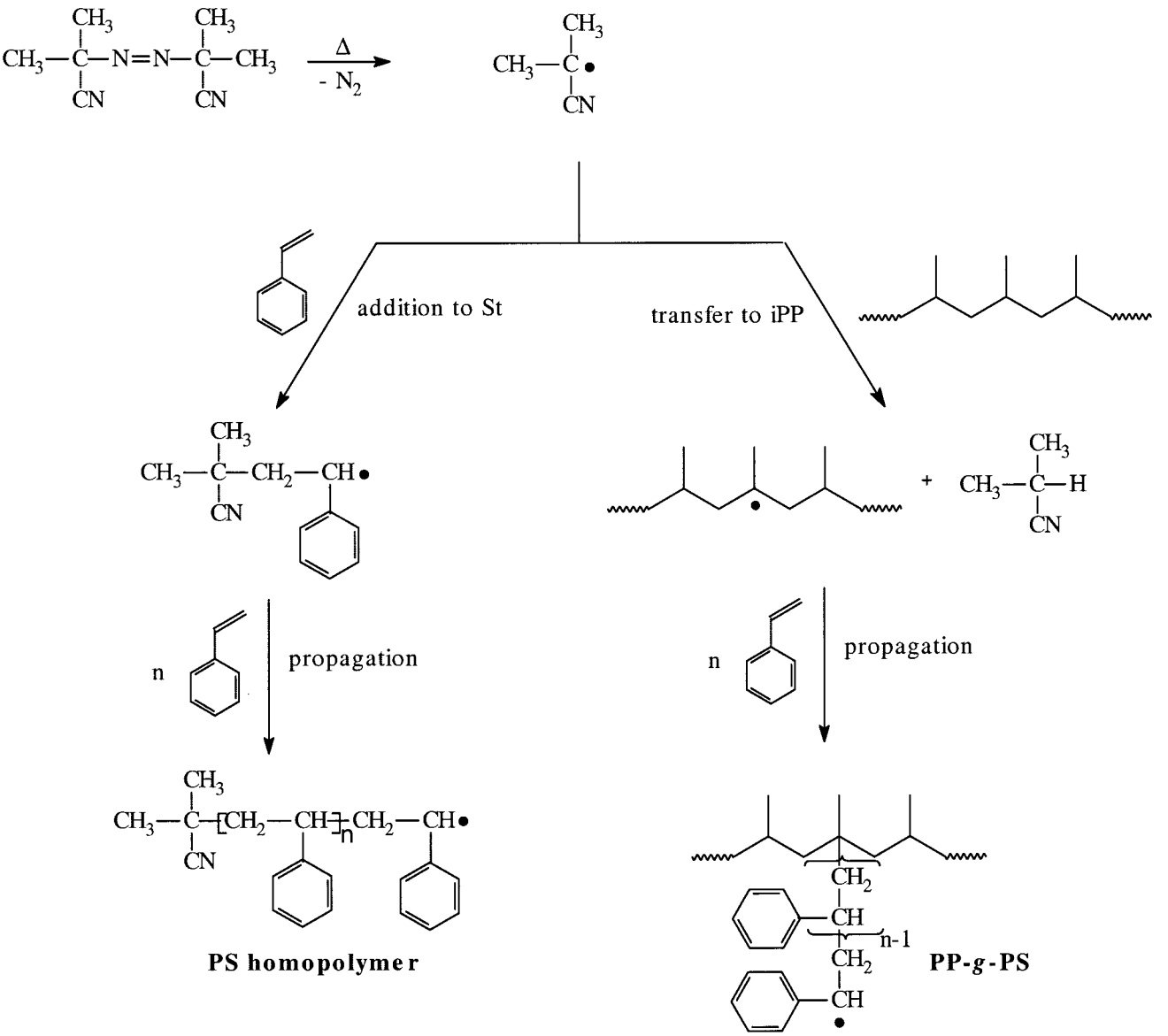

Scheme 3 Polymerization mechanism.

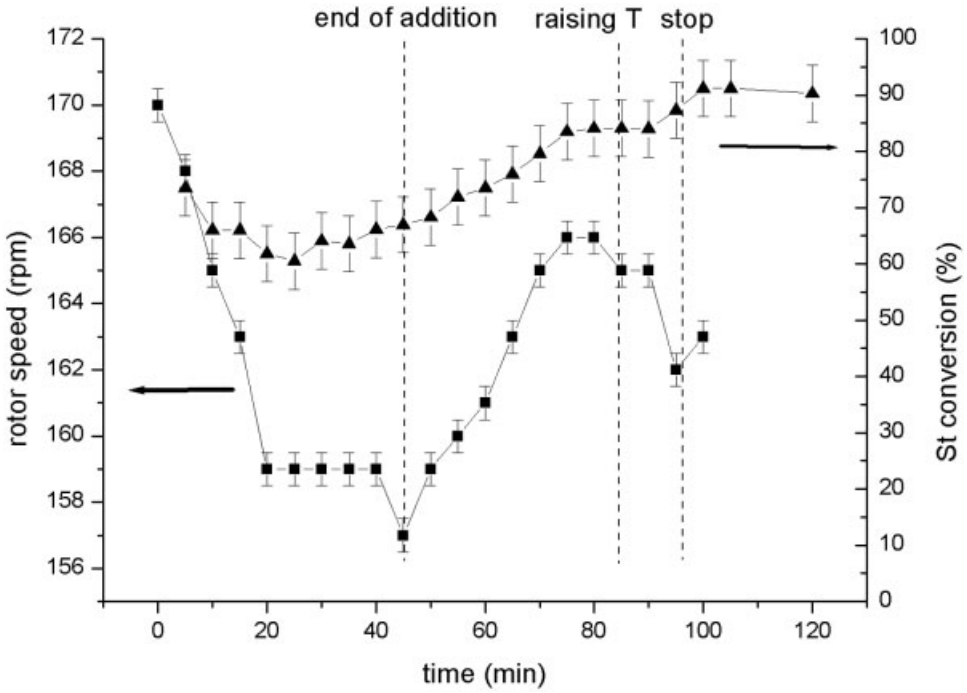

Figure 4 Rotor speed and styrene conversion as a function of time (data for iPP2). St conversion is calculated for every given time on the basis of the PS content and the St cumulative amount at that specific time.

iPP. At high AIBN contents, the primary radicals may easily transfer through hydrogen abstraction from iPP (Scheme 3), instead of adding St molecules and thus initiating the polymerization. In the absence of chain termination by transfer, as in the case of radical–bulk polymerization of St,[35] high values of the grafting efficiency should be measured at high AIBN contents.

In order to get some insight into the polymerization kinetics, the iPP2 experiment was repeated and at fixed times samples were removed from the reactor. The stirrer speed value, with the motor working at fixed power, gives an indirect and rather rough estimation of the system "viscosity". Figure 4 shows that the stirrer speed changes significantly during the polymerization.There is in fact an initial decrease (corresponding to a viscosity increase) during the addition time followed by an increase (corresponding to a viscosity decrease) during the reaction time. Finally, the speed decreases again (increase in viscosity) during the annealing step at 110°C. For each time the PS conversion is normalized to the amount of St added up to that point. It increases almost monotonously from about 70 to 90%. During the addition time new liquid St is added to the iPP powder. The sharp increase of the viscosity may in this case be related to the agglomeration/interaction of powder particles by the liquid monomer adsorbed on the surface. During the reaction step the viscosity decreases due to the conversion of St monomer into PS. Finally, in the annealing step there is again a viscosity increase due to the fact that PS polymerized at the surface of the iPP powder softens, because the temperature is above the glass transition of PS, resulting again in some particle aggregation.

The distribution of the formed PS in the iPP powder particles was investigated by Raman spectroscopy. It was indeed possible to obtain cross-sections of single particles (Fig. 5) and to record Raman spectra along the radius from the particle center to the surface. The ratio of the peak intensities at 1600 and 1260 cm^{-1}, characteristic of the PS and PP phases, respectively (I, intensity ratio), has been taken as a measure for the PS/PP composition ratio in every position. The resulting profile for iPP2 as a function of the distance from

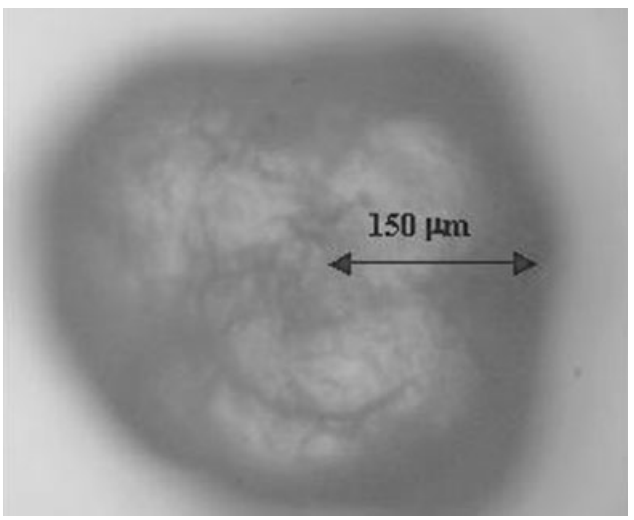

Figure 5 Cross-section optical image of iPP2 particle.

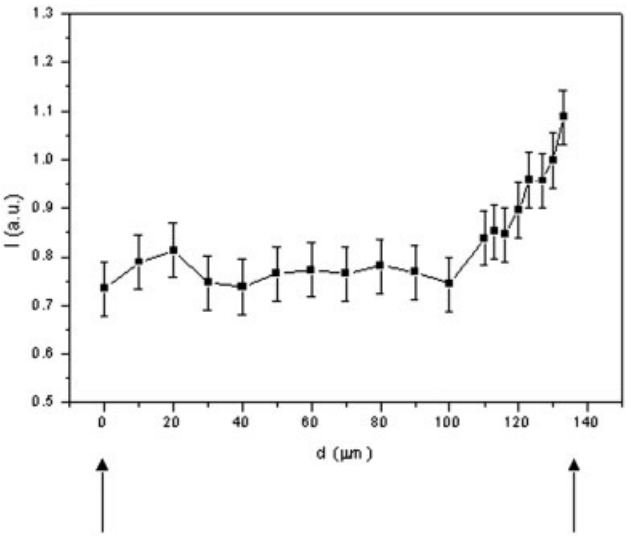

Figure 6 Raman profile of an iPP2 particle.

the particle center, given in Figure 6, clearly shows a homogeneous distribution of PS inside the particle, but a sharp increase of the PS content on approaching the particle edge. There is a kind of PS shell formed on the surface of the iPP particles upon polymerization in agreement with the increased viscosity in the annealing step.

A fractionation procedure (Scheme 2) was developed with the aim of separating the three polymeric species that in principle are present in the reaction products: iPP, PS, and iPP-*g*-PS. The procedure was first evaluated by iPP/PS blends obtained by physical mixing of the two polymer powders and by melt mixing in a miniextruder at 200°C (Table III). It can be concluded that the fractionation is almost quantitative and that no final residue is collected for these blends in which no graft copolymer is present. The FTIR characterization of the different fractions is also in agreement with the expected chemical composition (Scheme 2). The fractionation procedure was validated for the samples containing graft copolymer, because the latter may influence the solubility of the corresponding homopolymers.[36,37] The corresponding procedure has been applied to some of the prepared blends by varying the time of extraction (Table IV). It is noted that the percentage of the CH_2Cl_2 extracted fraction does not change significantly with time, indicating that all the free PS soluble in CH_2Cl_2 has been already extracted after 4 h. The amount of the residue of the *n*-octane extraction does not change significantly with time either, indicating that this fractionation step is also quantitative.

The above observations seem to indicate the validity of the fractionation procedure also in the case of the solid-state iPP/PS polymerized blends. However, the results of the FTIR characterization of the corresponding fractions were very surprising. As expected, the CH_2Cl_2 extracts display FTIR spectra typical of a PS. However, the residue of the *n*-octane extraction, which was expected to correspond to the graft copolymer, yielded spectra typical again of a pure PS. This indicates that the interpretation of the fractionation scheme has to be modified (Scheme 4) for the iPP/PS blends prepared by solid-state modification because the presence of two different kinds of PS homopolymer, of which only one (PS_1 in the scheme) is directly extractable in CH_2Cl_2, has to be taken into account. At this point, the question arises whether the graft copolymer, which was not isolated from the corresponding homopolymers, is actually formed during the polymerization. In this respect, it is observed that for all the synthesized iPP/PS blends (Table V) the total amount of extracted PS, that is, PS_1 plus PS_2, is always lower than or at best equal to the total PS amount determined by FTIR. This implies that in the *n*-octane soluble fractions some PS is present, which was confirmed by FTIR, and it is concluded that the PP-*g*-PS is soluble in *n*-octane. The overall extraction behavior can be explained by taking into account the formation of three different kinds of PS chains, which are located at the surface of the PP particles (PSs), in the pores (PSp), and in the amorphous (PSa) iPP phase (Scheme 5). It is noted that, from a macroscopic point of view, PSs can actually correspond to two different kinds of PS: PS on the surface of the macroparticle (which constitutes the shell detected by the Raman analysis) and PS in the large pores between the microparticles. In the course of the first extraction with CH_2Cl_2, only PSs is extracted (corresponding to PS_1 in Scheme 4). PSp cannot be extracted, due to the hindered accessibility of the solvent into the pores, and it remains as octane-"insoluble" (PS_2 in Scheme 4). In our hypoth-

TABLE III
Fractionation Results for Reference Blends Prepared by Powder Mixing (p) and Melt Processing (m)

Blend	Extr.CH_2Cl_2 (wt %)[a]	Extr. *n*-octane (wt %)[a]	Res. *n*-octane (wt %)[a]	Γ (%)[b]
iPP/PS 80/20 (p)	19.6	80.4	0.0	97
iPP/PS 70/30 (p)	28.4	71.6	0.0	96
iPP/PS 80/20 (m)	20.3	79.7	0.0	98
iPP/PS 70/30 (m)	29.2	70.8	0.0	99

[a] Percentages were renormalized to 100% after extraction.
[b] Extraction efficiency calculated according to eqs. (4) and (5).

TABLE IV
Fractionation Results for Solid-State Polymerized iPP/PS Blends as a Function of the Extraction Time

Blend	Time (h)	PS (wt %)[a]	Extr. CH_2Cl_2 (wt %)[b]	Res. *n*-octane (wt %)[c]
	4		0.6	
iPP20	5	7.7	0.4	
	10		0.4	
	4		0.6	
iPP21	5	18.3	0.4	
	10		0.5	
	8			2.1
iPP19	12	25.7		1.9
	16			2.4

[a] Determined by FTIR.
[b] Corresponding to the first extraction of the modified powder by CH_2Cl_2.
[c] Corresponding to the extraction of the CH_2Cl_2 residue by *n*-octane.

esis the PSs, which constitutes the free PS in the large pores between the microparticles, is also extracted with CH_2Cl_2. PSa, which is intimately mixed with the iPP, is extracted in *n*-octane and it is most probably constituted by grafted chains.[21,38]

TABLE V
Fractionation Results

Run	PS (wt %)	Fractionation PS_1	Fractionation PS_2	Fractionation PP/PP-g-PS	Results Φ (%)[a]	Results Γ (%)[a]
iPP13	0.0	0.0	0.0	100.0	0	98
iPP16	0.0	0.0	0.0	100.0	0	99
iPP7	3.4	1.2	0.5	98.3	50	95
iPP21	7.7	0.4	0.0	99.6	93	97
iPP1	18.3	1.0	0.0	99.0	94	98
iPP8	18.4	0.8	0.0	99.2	96	96
iPP22	19.3	1.8	1.5	96.7	83	93
iPP4	14.6	2.0	3.0	95.0	66	98
iPP24	14.2	1.5	3.9	94.6	62	96
iPP9	15.7	1.2	3.0	95.8	73	98
iPP12	13.6	2.6	5.3	93.1	42	97
iPP2	28.4	7.8	12.1	80.1	30	97
iPP11	28.9	6.9	10.6	82.5	39	94
iPP18	23.0	7.1	2.9	90.0	56	98
iPP10	23.8	5.2	1.6	93.2	71	98
iPP19	25.7	5.3	2.1	92.6	71	97

[a] Grafting and extraction efficiencies calculated according to eqs. (3)–(5).

This explanation is supported by some additional observations. First, reversing the order of the extractions, that is, first extracting with *n*-octane and then

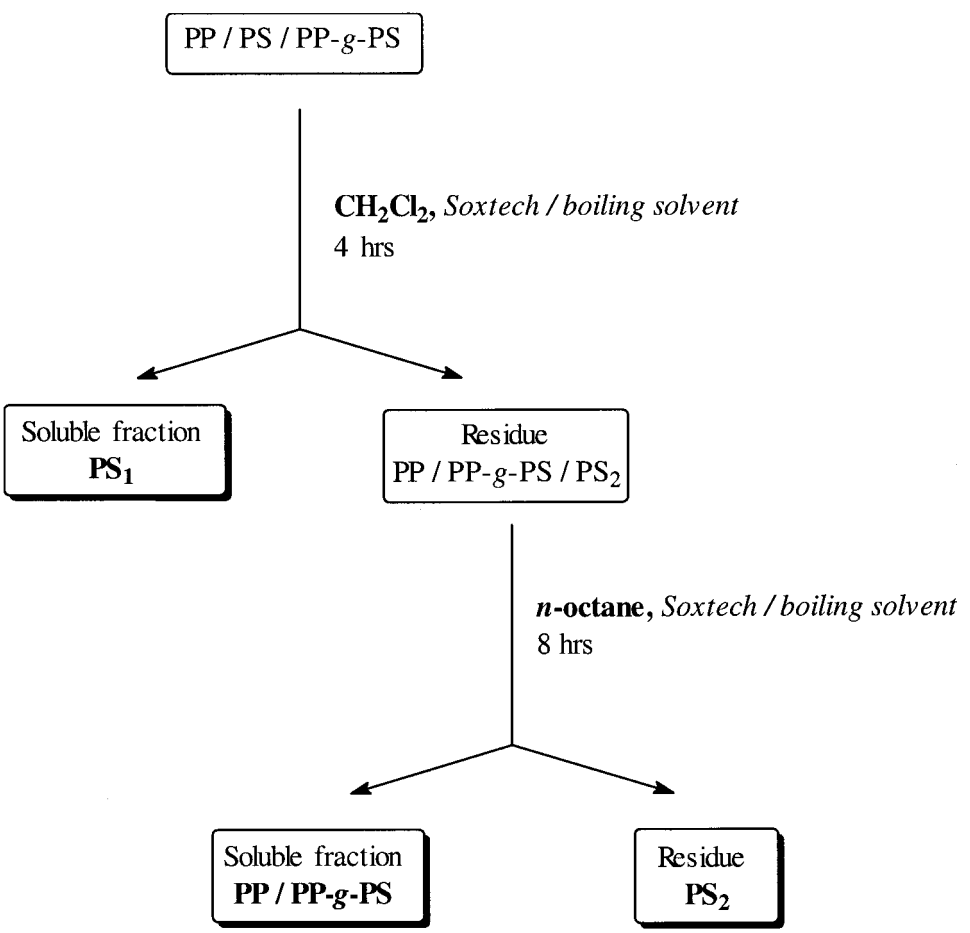

Scheme 4 Fractionation procedure: real results.

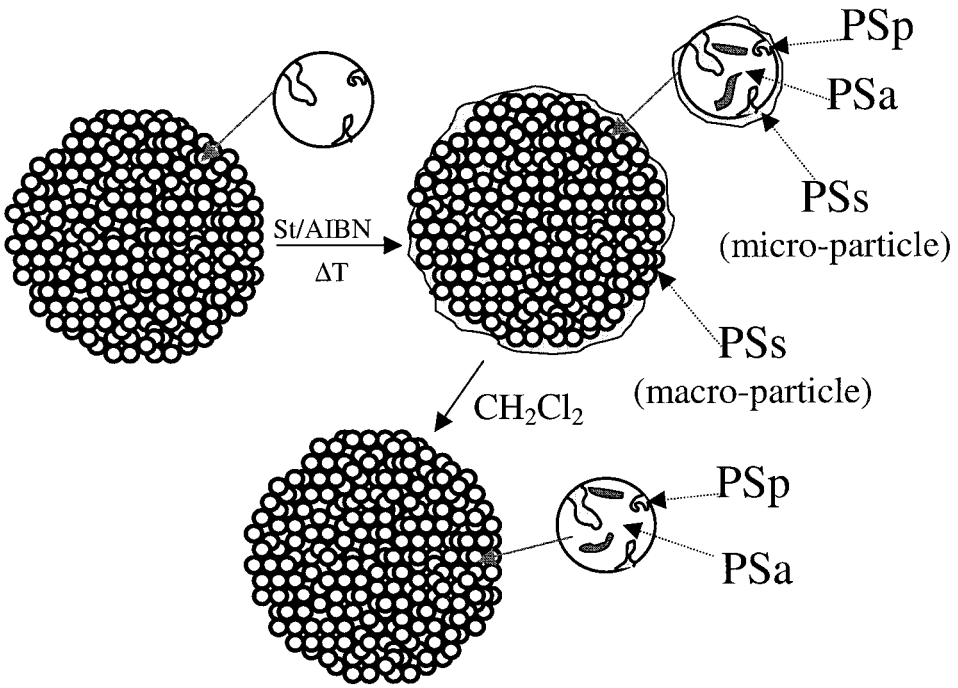

Scheme 5 Rationalization of the fractionation procedure.

the corresponding residue with CH_2Cl_2, yields one soluble PS phase. The amount of this PS extract is equal, within the experimental error, to the combined PS_1 and PS_2 amounts in the direct scheme. Secondly, Raman spectra recorded along the particle radius after extraction by CH_2Cl_2 (Fig. 7) do not show any excess of PS at the particle surface in contrast to the original sample particle. Finally, surface area (S_{BET}) measurements (Table VI) indicate a net reduction of the overall surface area in the polymerized iPP2 experiment (from 0.068 to 0.017 m^2/g). This can be explained by the hindered accessibility of krypton probe in the particle by the PSs shell. On the other hand, upon extraction by CH_2Cl_2, S_{BET} increases again to a value close to that of pure iPP (0.055 m^2/g), strongly suggesting that this extraction is able to selectively remove PSs.

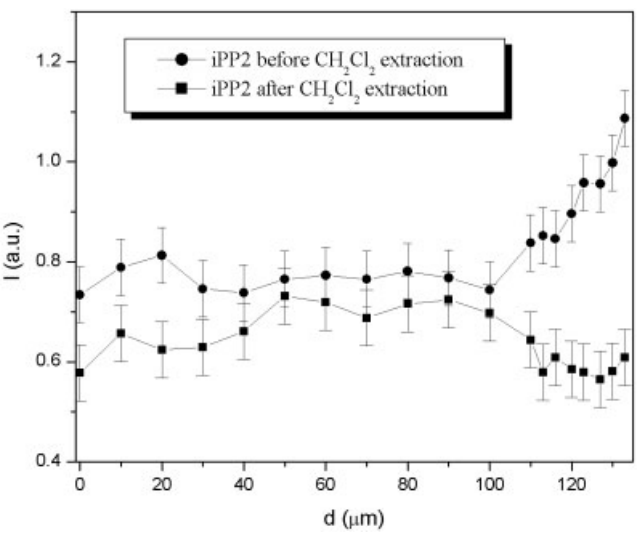

Figure 7 Raman spectra of iPP/PS particle after extraction by CH_2Cl_2.

In order to get more insight into the PS distribution in the modified iPP particles, solid-state spin diffusion NMR experiments have been performed on the iPP2 sample before and after extraction by CH_2Cl_2. The proton relaxation time values (Table VII) both in the laboratory (T_1) and in the rotating frame ($T_{1\rho}$)[39,40] display some interesting characteristics. The T_1 and $T_{1\rho}$ values for the PP and PS phase are significantly different in the iPP2 particles before extraction, clearly indicating that the two components are phase-separated and display very poor miscibility. In the extracted samples the T_1 values approach each other, while the $T_{1\rho}$ remain unchanged. This indicates that the two components are still phase-separated but more intimately mixed than in the particles before extraction.

These observations are in perfect agreement with the PS distribution proposed in Scheme 5. Upon extraction by CH_2Cl_2 the free PS on the particle surface is removed, leaving some free PS in the pores (not intimately mixed with iPP) and the PS in the amorphous phase of iPP (probably constituted of grafted chains intimately mixed with iPP).

TABLE VI
Surface Area Measurements

Sample	S_{BET} (m^2/g)
iPP	0.068
iPP2	0.017
iPP2 (after CH_2Cl_2 extraction)	0.055

TABLE VII
Solid-State NMR Results: Relaxation Times

	T_1 (iPP) (s)	T_1 (PS) (s)	$T_{1\rho}$ (PP) (ms)	$T_{1\rho}$ (PS) (ms)
PP	1.1			
PS		3.5		
iPP2	1.0	1.5	37	14
iPP2 (res. CH_2Cl_2)	0.9	1.1	32	15

Although the fractionation procedure does not allow a complete separation of the graft copolymer from the corresponding homopolymers, it still allows the calculation of the grafting efficiency (Φ in Table V) according to the following equation:

$$\Phi = \frac{PS_{tot}\,(wt\,\%) - PS_{extr}\,(wt\,\%)}{PS_{tot}\,(wt\,\%)} \times 100 = \left(1 - \frac{PS_{extr}\,(wt\,\%)}{PS_{tot}\,(wt\,\%)}\right) \times 100 \quad (7)$$

where PS_{tot} is the total PS content determined by FTIR and PS_{extr} the weight content of all "extractable", being the sum of the CH_2Cl_2 soluble fraction and the *n*-octane residue. Grafting efficiencies from 30% up to 90% are found. A simple error propagation scheme,[30,31] together with the estimation of the absolute error on both PS_{tot} and PS_{extr}, yields an average absolute error on Φ of approximately 6%. The plot of the grafting efficiency as a function of the AIBN content at fixed iPP/St ratio and feeding rate, as given in Figure 8, displays a minimum at approximately 1 wt % of AIBN with respect to the St amount. The plot of the formed free PS_1 and PS_2 as a function of the AIBN content (Fig. 9) shows in both cases a maximum around 1 wt % of AIBN. According to the representation in Scheme 5 and the literature,[41,42] the amount of PS_2, as compared to that of PS_1, may be an indirect measure of relative diffusion/polymerization rates. At low AIBN content, the amount of PS_2 is larger than that of PS_1, so the diffusion rate seems to prevail over the polymerization rate. This results in high Φ values, because the formation of the grafted chains is strictly limited by the diffusion and absorption of the monomer into the iPP amorphous phase.[20,21,38] At high AIBN contents the influence of diffusion seems to be much less than in the previous case, because the amount of PS_2 is lower than that of PS_1. However, the number of primary radicals is so high that the chance of hydrogen abstraction is much higher than that of addition to St. Anyway, the observed behavior strikingly confirms the hypothesis of high Φ values for high AIBN contents formulated when discussing the conversion dependence in Figure 3.

The plot of the grafting efficiency as a function of the feeding rate (Fig. 10) displays a broad maximum at around 0.8–1.5 pph/min. In this case the influence of

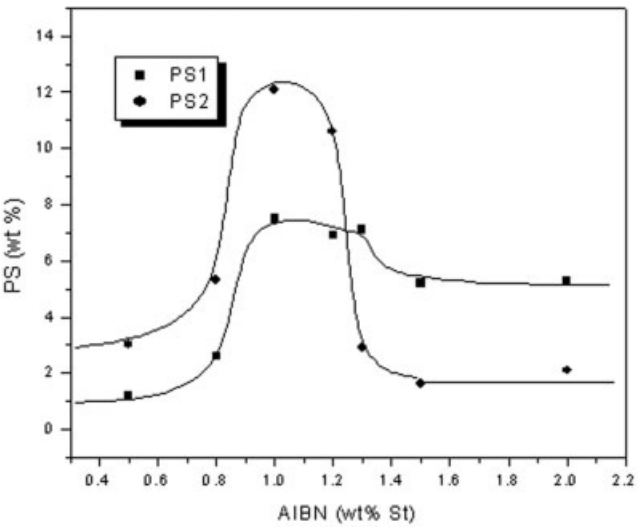

Figure 9 PS_1 and PS_2 amounts as a function of AIBN concentration in feed.

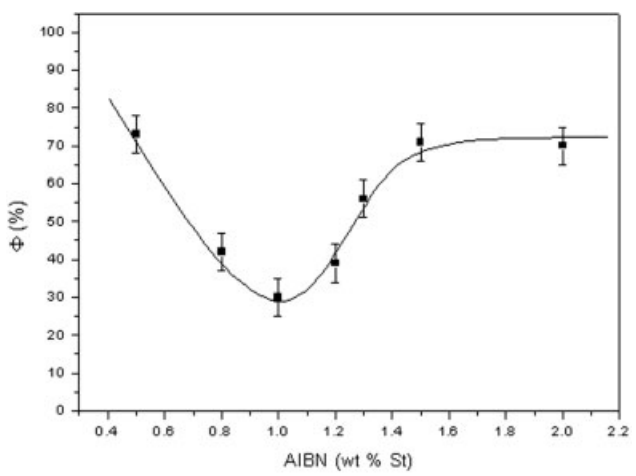

Figure 8 Grafting efficiency (Φ) as a function of AIBN concentration. iPP/St 70/30 wt/wt; r_{add} = 1.0 pph/min iPP.

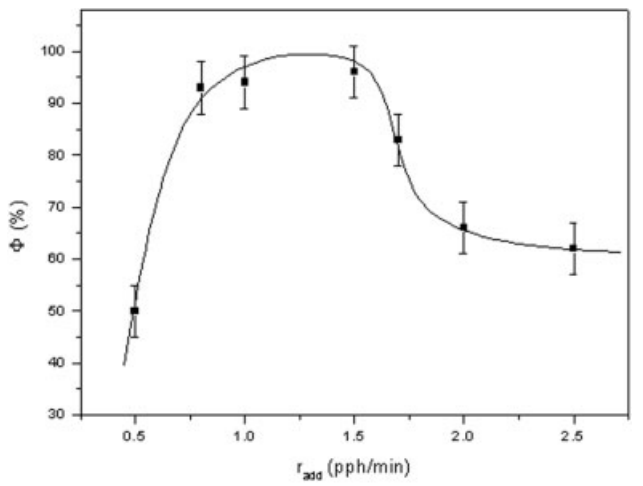

Figure 10 Grafting efficiency (Φ) as a function of feeding rate (r_{add}). iPP/St 80/20 wt/wt; AIBN 1 wt % St.

the diffusion/polymerization rates could not be inferred by the relative amounts of formed PS_1 and PS_2, because the measured values do not differ significantly within the specified error limit (6%).

CONCLUSIONS

The chemical and morphological aspects of the solid-state graft polymerization of St onto iPP have been studied. Clear trends in the St conversion as a function of the AIBN content and the feeding rate were observed and tentatively explained on the basis of the diffusion/polymerization rates balance. The St conversion may reach completeness by optimizing the experimental conditions.

A study on the distribution of the newly formed PS in the iPP particles clearly showed the formation of PS on the surface, in the pores, and in the amorphous phase of the iPP microparticle. This distribution has a pronounced and unusual influence on the selective solvent extractions: two kinds of free PS were selectively separated. The schematic model for the distribution of the PS phase has been proposed and validated on the basis of the extraction behavior, Raman analysis, and the surface area measurements. The extractions did not allow the neat separation of the graft copolymer, but its presence could be indirectly calculated from the fractionation data and directly demonstrated with solid-state NMR measurements. The grafting efficiency shows a maximum as a function of the feed composition, which is consistent with the results of the St conversion and with the hypothesis formulated on the polymerization/diffusion rates balance.

Although the experimental data were carefully recorded and the explanation of the experimental trends is most probably accurate, a theoretical model for the polymerization of St under these peculiar conditions is needed in order to better understand and rationalize the observed behavior. Moreover, the morphological characterization of the reaction product and the stability of the morphology upon melt processing are currently under investigation.

H. Repin (DSM Research), W. Bruls (DSM Research), F. op den Buijsch (DSM Research), and J.D. van Loon (Basell) are acknowledged for the very helpful discussions. F. van de Boogaard and E.M. van Oers are especially acknowledged for the setting up of the solid-state reactor and the help in the solid-state NMR experiments, respectively. P. van Oeffelt (DSM Research) is acknowledged for the BET measurements.

References

1. Citovicki, P.; Mikulasova, D.; Chrastova, V. Eur Polym J 1976, 12, 627.
2. Citovicki, P.; Mikulasova, D.; Chrastova, V.; Benc, G. Eur Polym J 1977, 13, 655.
3. Citovicki, P.; Mikulasova, D.; Chrastova, V.; Reznicek, J.; Benc, G. Eur Polym J 1977, 13, 661.
4. Rengarajan, R.; Vicic, M.; Lee, S. Polymer 1989, 30, 933.
5. Rengarajan, R.; Vicic, M.; Lee, S. J Appl Polym Sci 1990, 39, 1783.
6. Rengarajan, R.; Parameswaran, V. R.; Lee, S.; Vicic, M.; Rinaldi, P. L. Polymer 1990, 31, 1703.
7. Lee, S.; Rengarajan, R.; Parameswaran, V. R. J Appl Polym Sci 1990, 41, 1891.
8. Borsig, E.; Hrckova, L. J Macromol Sci-Pure Appl Chem 1994, A31, 1447.
9. Lazar, M.; Hrckova, L.; Fiedlerova, A.; Borsig, E.; Rätzsch, M.; Hesse, A. Angew Makromol Chem 1996, 243, 57.
10. Galli, P. J Macromol Sci-Pure Appl Chem 1999, A36, 1561.
11. Galli, P. Macromol Symp 1994, 78, 269.
12. Galli, P. Prog Polym Sci 1994, 19, 959.
13. Galli, P.; Haylock, J. C.; Albizzati, E.; DeNicola, A. Macromol Symp 1995, 98, 1309.
14. Galli, P. J Macromol Sci-Phys 1996, B35, 427.
15. Galli, P.; Collina, G.; Sgarzi, P.; Baruzzi, G.; Marchetti, E. J Appl Polym Sci 1997, 66, 1831.
16. Galli, P. J Macromol Sci -Pure Appl Chem 1999, A36, 1797.
17. DeNicola, A. J.; Guhaniyogi, S. EP Pat. EP0439079 A2 (1991).
18. Galli, P.; DeNicola, A. J.; Smith, J. A. EP Pat. EP0437808 (1991).
19. Ferraro, A.; Fava, R. A.; VanEvery, K. W. Compalloy '93, 1993, 71.
20. Rätzsch, M.; Bucka, H.; Wohlfahrt, C. Angew Makromol Chem 1995, 229, 145.
21. Rätzsch, M.; Bucka, H.; Hesse, A.; Arnold, M. J Macromol Sci-Pure Appl Chem 1996, A33(7), 913.
22. Rätzsch, M.; Hesse, A.; Bucka, H. DE Pat. DE4435534 (1996).
23. Rätzsch, M.; Hesse, A.; Bucka, H. U.S. Pat US5585435 (1996).
24. Panzer, U.; Bucka, H.; Hesse, A.; Rätzsch, M.; Reichelt, N. EP Pat. EP0792894 (1997).
25. Rätzsch, M.; Hesse, A.; Bucka, H.; Reichelt, N.; Panzer, U. DE Pat. DE19607430 (1997).
26. Reichelt, N.; Panzer, U.; Hesse, A.; Bucka, H.; Rätzsch, M. EP Pat. EP0879830 (1998).
27. Reichelt, N.; Rätzsch, M.; Heikin, S.; Ivanchev, S.; Mesh, A.; Fodorova, N. EP Pat. EP0964011 (1999).
28. Roelands, D. Graduation Report, Eindhoven University of Technology, The Netherlands, 1999.
29. Gregg, S. J.; Sing, K. S. W. Adsorption, Surface Area and Porosity, 2nd ed.; Academic Press: London, 1982.
30. Youden, W. J. Statistical methods for chemists; John Wiley and Sons: New York, 1951.
31. Montgomery, D. C. Design and Analysis of Experiments, 5th ed.; John Wiley and Sons: New York, 2001.
32. Picchioni, F.; Goossens, J. G. P.; van Duin, M. Macromol Symp 2001, 176, 245.
33. Davenport, W.; Michalak, L.; Malmstrom, E.; Mate, M.; Kurdi, B.; Hawker, C. J. Macromolecules 1997, 30, 1929.
34. Daroux, M.; Zamani, H.; Greffe, J. L.; Bordet, J. Chem Eng J 1981, 22, 12.
35. Moad, G.; Solomon, D. H. The Chemistry of Free Radical Polymerization; Elsevier Science Ltd.: 1995.
36. Passaglia, E.; Picchioni, F.; Aglietto, M.; Ruggeri, G.; Ciardelli, F. Tr J Chem 1997, 21, 262.
37. Passaglia, E.; Aglietto, M.; Ruggeri, G.; Picchioni, F. Polym Adv Technol 1998, 9, 273.
38. Borsig, E.; Lazár, M.; Fiedlerová, A.; Hrčková, L.; Rätzsch, M.; Marcinčin, A. Macromol Symp 2001, 176, 289.
39. Schmidt-Rohr, K.; Spiess, H. W. Multidimensional solid-state NMR and polymers: Academic Press: 1994.
40. Simonutti, R.; Mariani, A.; Sozzani, P.; Bracco, S.; Piacentini, M.; Russo, S. Macromolecules 2002, 35, 3563.
41. Giroux, T. A.; Song, C. Q. Polym Prepr 1999, 40, 130.
42. Song, C. Q.; Giroux, T. A. Polym Prepr 1999, 40, 111.